BJGEO
Brazilian Journal of Geology

Facies architecture and volcanological aspects of silicic rocks from the Palmas plateau, Brazil

Luanna Chmyz[1]* , Eleonora Maria Gouvêa Vasconcellos[1] , Otavio Augusto Boni Licht[1]

Abstract

The nature of the extensive silicic units of the Paraná Igneous Province is still heavily debated. The silicic rocks that outcrop in the Palmas plateau (Southwestern Parana State) show aphyric texture and $TiO_2 < 0.86\%$, being classified as Palmas-type rhyolites. Physical volcanology criteria are used here to constrain their origin. Textural and structural variations are observed in these rocks, resulting in the description of nine lithofacies: pitchstone; banded vitreous rhyolite; aphanitic rhyolite; rhyolite with planar disjunctions; massive rhyolite; compositionally banded rhyolite; amygdaloid rhyolite, rhyolite with quartz levels, and altered rhyolite. Folded compositional banding associated with volcanic conduits, well-defined lobes and basal autobreccias attest to an effusive origin for most lithofacies. They occur as domes or extensive tabular bodies, fed by volcanic conduits. For both domes and tabular units, the faciological sequence involves (from bottom to top): altered rhyolite; aphanitic rhyolite or rhyolite with tightly-spaced planar disjunctions; monotonous rhyolite with decimetric-spaced planar disjunctions; and top portions with fast cooling features. Only banded vitreous rhyolite differs due to the presence of shards and gas-escape pipes, aspects that imply in a pyroclastic nature. Therefore, a secondary pyroclastic flow created by lava collapse is suggested as its origin, although further studies are required.

KEYWORDS: silicic rocks; rhyolites; lava domes; effusive rhyolites; Paraná continental flood basalts.

INTRODUCTION

The origin of extensive silicic units (either effusive or pyroclastic) is still fairly controversial. The difficulty in establishing the origin of these rocks lies in the contentious genesis of large silicic flows and the generally inaccurate characterization of rheomorphic ignimbrites (Milner *et al.* 1992, Henry and Wolff 1992, Manley 1996, Polo *et al.* 2018b). The latter is due to the loss of pyroclastic textures as fragments weld at high flow temperatures, as verified in rheomorphic processes (Branney and Kokelaar 1992, Andrews and Branney 2011). Thus, pyroclastic rocks may have typical features of effusive lithotypes. Moreover, changes in the eruption style as a volcanic episode pursues may increase the complexity of silicic units (Bryan *et al.* 2000). Therefore, to achieve a more refined understanding of the processes that originated large silicic bodies, each volcanic unit must be studied individually.

As for the silicic rocks of the Paraná Igneous Province (PIP, southern Brazil; Fig. 1), those outcropping in the Palmas plateau (in the central portion of the province) are still subject to debate. The widespread occurrence of Palmas-type units,

fairly uncommon for silicic lavas, motivated the proposition of different genetic models for those rocks. Because of its large dimensions — more than 60 km in extension —, the rock bodies would, according to Bellieni *et al.* (1986), correspond to ignimbrites, despite the absence of typical textures. A similar origin is proposed by Roisenberg (1989), Philipp *et al.* (1994), and Luchetti *et al.* (2018b). Conversely, other authors attribute an effusive origin to the voluminous silicic volcanites of the PIP. In this case, the abnormally high effusion temperature (930–1,010°C) and low H_2O content (~1–2 wt.%) would be responsible for the low viscosity values (Nardy 1995, Simões *et al.* 2018, Polo *et al.* 2018a) and, consequently, the widespread distribution of the rocks. Effusive models involve extensive tabular flows and lateral coalescence of domes and coulées (Umann *et al.* 2001, Waichel *et al.* 2012, Lima *et al.* 2012, Besser *et al.* 2018, Polo and Janasi 2014, Polo *et al.* 2018b, Guimarães *et al.* 2018a, 2018b, Benites *et al.* 2020). Some of these authors (*e.g.*, Umann *et al.* 2001, Guimarães *et al.* 2018a), however, do not disregard the presence of volumetrically subordinate pyroclastic rocks among the sicilic volcanites of the province.

In this sense, this paper aims to contribute to the knowledge of silicic rocks from the Palmas plateau, based mainly on physical volcanology aspects (*i.e.*, lithofaciological, morphological, and architectural characterization of the silicic bodies), as well as to present new lithogeochemical data for these rocks.

[1]Universidade Federal do Paraná – Curitiba (PR), Brazil. E-mails: chmyz@ufpr.br, eleonora@ufpr.br, otavio.licht@gmail.com

*Corresponding author.

GEOLOGICAL SETTING

In the southern Brazilian Platform, the voluminous tholeiitic magmatism that preceded the opening of the South Atlantic
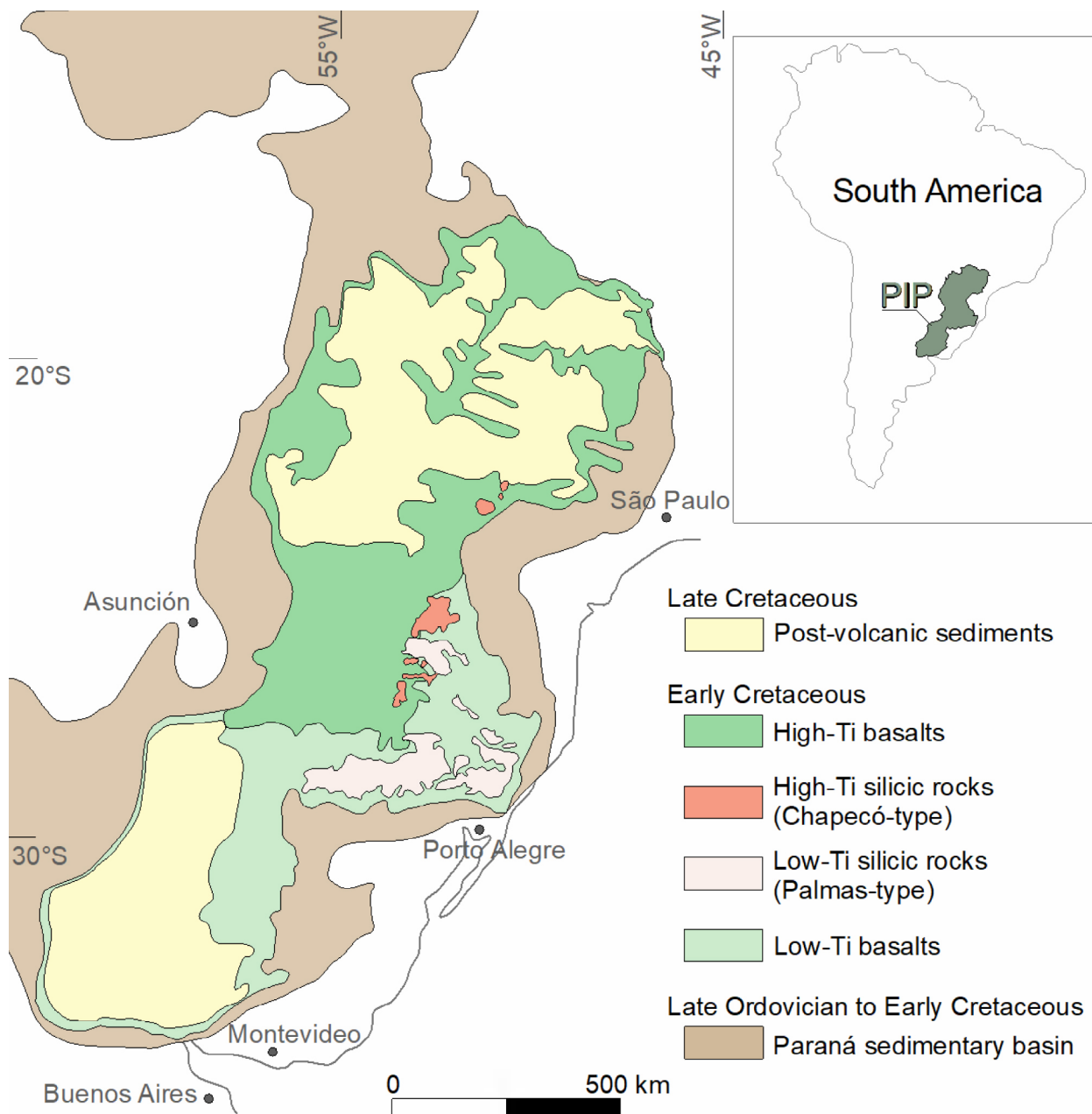
Figure 1. Simplified geologic map of the Paraná Igneous Province (Polo *et al.* 2018b and references therein) showing the spatial distribution of Ti-low and Ti-high volcanic rocks.

Ocean culminated in an extensive continental flood basalt (CFB) event, the PIP, with Early Cretaceous ages (Marques and Ernesto 2004). The PIP is the sixth-largest Meso-Cenozoic large igneous province on Earth (Machado *et al.* 2018) and mostly consists of tholeiitic basalts (90%) with minor andesites (7%) and rhyodacites/rhyolites (ca. 3%) (Bellieni *et al.* 1986), totalizing an estimated volume of at least 600,000 km³ of volcanic rocks (Frank *et al.* 2009).

Bellieni *et al.* (1984) classified the Paraná CFB into high-TiO$_2$ (average 3.4 wt.%) and low-TiO$_2$ (average 1.4 wt.%) basalts. According to those authors, such a division is also mirrored in other geochemical and isotopic particularities of the Paraná CFB (*e.g.*, Sr isotopic ratios, incompatible element contents), as well as in their spatial distribution: while high-Ti basalts dominate the north of the province, low-Ti basalts are mainly limited to the southern area (Fig. 1). Subsequently, Peate *et al.* (1992)

identified six basaltic magma-types in the PIP based on their geochemical characteristics, though still considering the TiO$_2$ division: the low-Ti Gramado, Esmeralda, and Ribeira types and the high-Ti Urubici, Pitanga, and Paranapanema types.

Despite the predominance of basic types, some silicic volcanic rocks outcrop in the southern and northern parts of the PIP, respectively classified into Palmas- (low TiO$_2$; ca. 0.6-1.2 wt.%) and Chapecó- (high TiO$_2$; ca. 0.9-1.6 wt.%) types (Bellieni *et al.* 1986, Peate *et al.* 1992, Garland *et al.* 1995, Nardy *et al.* 2008). Figure 1 highlights that the spatial predominance of high-Ti volcanites in the northern portion of the PIP and low-Ti rocks in the south is observed for both basic and silicic types. Chapecó- and Palmas-types also differ from each other by other major (SiO$_2$ and P$_2$O$_5$) and incompatible element contents (Zr, Ba, Sr), as well as by their different isotopic ratios (Garland *et al.* 1995).

These silicic rocks correspond to extensive and sparsely vegetated plateaus related to highlands (the Palmas-type rocks covering from 241 to 8,929 km^2 and the Chapecó-type, from 13 to 1,776 km^2) (Nardy *et al.* 2008). Both types can be easily recognized, even at fieldwork (Melfi *et al.* 1988, Nardy *et al.* 2008): while Palmas rocks are aphyric to subaphyric with "salt and pepper" textures where altered, Chapecó lithotypes are often porphyritic with plagioclase phenocrysts up to 20 mm. Petrographic and geochemical criteria guided the classification of the Palmas-type silicic rocks into subgroups (Peate *et al.* 1992, Garland *et al.* 1995, Nardy *et al.* 2008, Polo *et al.* 2018b): rhyolites Santa Maria (P$_2$O$_5$ ≤ 0.21%) and Clevelândia (0.21% < P$_2$O$_5$ ≤ 0.23%), both subtypes with low TiO$_2$ (TiO$_2$ ≤ 0.87%); Caxias do Sul (0.91% < TiO$_2$ < 1.03%; 0.25% < P$_2$O$_5$ < 0.28%), Anita Garibaldi (1.06% < TiO$_2$ < 1.25%; 0.32% < P$_2$O$_5$ < 0.36%) and Jacuí (1.05% < TiO$_2$ < 1.16%; 0.28% < P$_2$O$_5$ < 0.31%) dacites, all of them presenting comparatively higher TiO$_2$ (≥ 0.90%).

Recently, Licht (2018) revises the classification of the extrusive rocks of the PIP and distinguishes 16 chemical types (according to their SiO$_2$, Zr, TiO$_2$, and P$_2$O$_5$ contents), each of them presenting a particular composition and geographic distribution. These aspects, along with geochronological data, are used by Licht (2018) to establish a spatial and temporal model for the PIP, proposing different evolutions for its southern and central-northern portions. That classification was further detailed by Gomes *et al.* (2018) for some basic-types.

ANALYTICAL METHODS

For the present study, fieldwork was carried out in the Palmas plateau aiming at the characterization of textural, structural, and morphological features of the silicic lithotypes (UTM coordinates of outcrops locations are reported in Supplementary Material A), as well as at the collection of samples for laboratory analysis. The investigated areas (Fig. 2) were selected based on previous geological mapping of the Serra Geral Group performed by Minerals of Paraná S/A (MINEROPAR). 58 petrographic thin sections of selected samples were provided for the present study by MINEROPAR. Representative samples of different lithofacies were sent to ACME Analytical Laboratories LTD in Canada for the determination of major
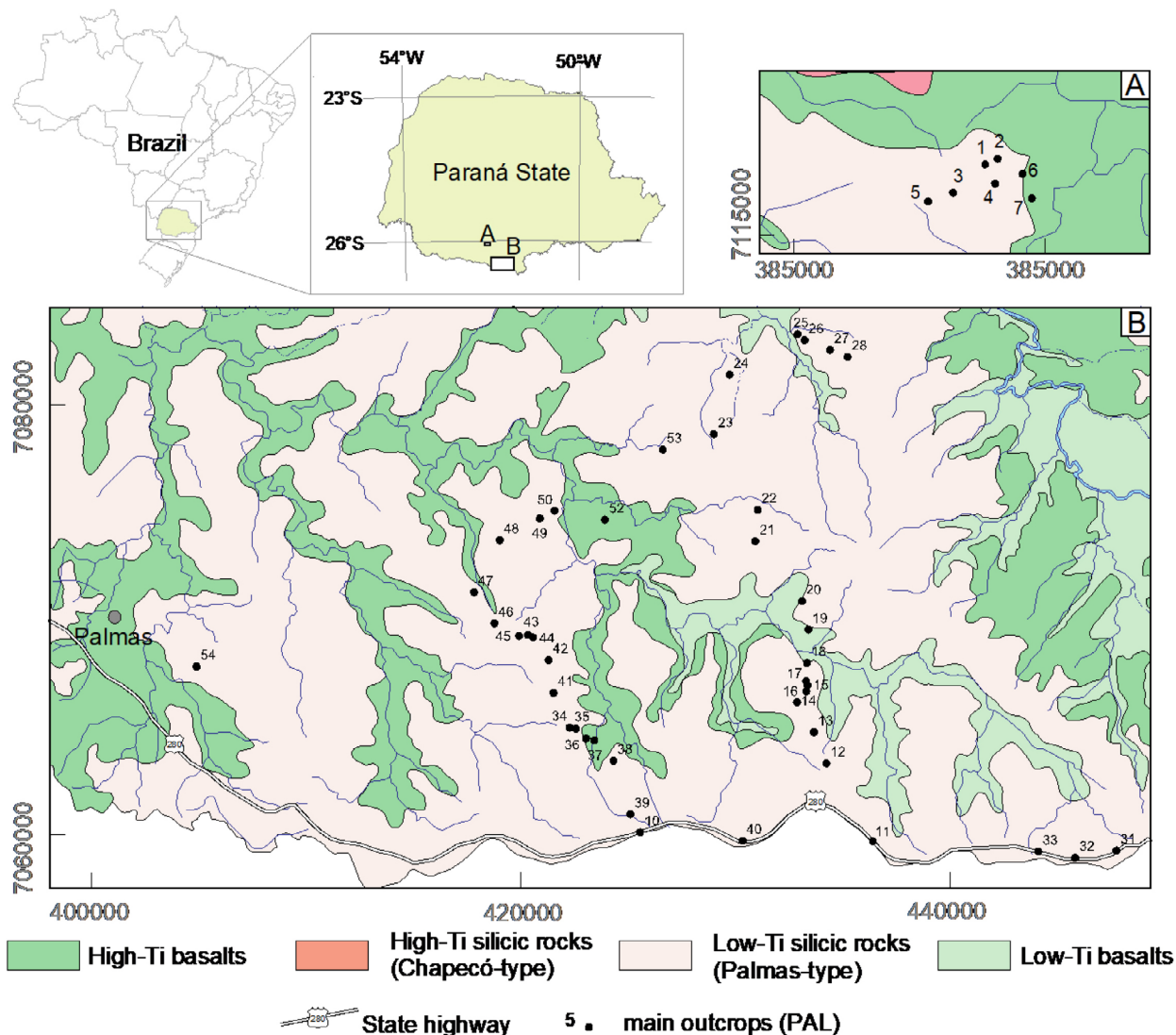
Figure 2. Geological map of the studied areas with the location of the investigated outcrops (geological units simplified from Licht and Arioli 2018, and topographic base from MINEROPAR 2005).

oxides by X-ray fluorescence and rare earth and trace elements by ICP-MS Plasma. Samples were analyzed by scanning electron microscopy (JEOL JSM-6010LA InTouchScope™) coupled with energy-dispersive X-ray Spectrometry by both secondary and back-scattered electron emission at the *Laboratório de Análise de Minerais e Rochas* (LAMIR) of the Universidade Federal do Paraná. For the latter, both *in natura* rock samples and thin sections were metalized with carbon. Four samples were submitted to cathodoluminescence essays for characterization of volcanic glass, using a CITL Mk5-2 microscope coupled to a conventional optical microscope.

RESULTS

Local geology and facies characterization

To better understand the processes that gave origin to the volcanogenic sequences of the Palmas plateau, a faciological characterization was approached. Lithotypes are then classified in terms of volcanic lithofacies following the definition of Németh and Martin (2007). According to those authors, volcanic lithofacies are well-defined, usually mappable rock units with particular textural, structural, and compositional features, which may serve as indicative of their formation processes.

The Palmas plateau occupies ca. 4,000 km² nearby the homonymous municipality, in the southwestern portion of Paraná State. Basaltic lava flows also occur in the studied areas, overlapped by the investigated silicic sequences (Figs. 2A and 2B). Field observation and petrographic analysis led to the identification of nine silicic lithofacies, as summarized in Table 1. Overall, these rocks show aphyric texture (a typical Palmas-type feature) but differ in terms of:

- proportions of glassy matrix and crystalline phases (*P*, pitchstone; *Rvb*, banded vitreous rhyolite);
- granulation (*Raf*, aphanitic rhyolite);

- structural characteristics (*Rd*, rhyolite with planar disjunctions; *Rm*, massive rhyolite; *Rb*, compositionally banded rhyolite; *Ram*, amygdaloid rhyolite; *Rq*, rhyolite with quartz levels).

Particularly, *Ral* (altered rhyolite) forms intensely altered reddish-orange horizons thought, in their majority, to be originally composed of volcanic glass.

Among the observed structures, planar disjunctions (also named horizontal columnar joints, Rossetti *et al.* 2018) are the most common (*Rd*, *Raf*, *Ram*, *Ral*, *Rq*, and *P* lithofacies) and are characterized by continuous, centimetric to decimetric detachment levels (Fig. 3A). Disjunctions are usually parallel or sub-parallel to each other, although lenticular shapes are also present. There may be slight undulation, with local gentle symmetrical folds. The *Rq* facies, in particular, bears discontinuous, occasionally truncated quartz levels parallel to disjunctions.

The flow banding described in *Rb*, *Rvb*, and some *Raf* samples are characterized by interleaving light and dark levels that differ in glassy content. The bands are parallel to sub-parallel to each other and may be folded, forming intrafolial (Fig. 3B), open, gentle, close, cusp, or sheath folds.

Although amygdales are only occasionally present in most lithofacies, in *Ram* and *Ral* they account for up to 35% of the total rock volume. In these cases, the amygdales are generally flattened parallel to the planar disjunction and aligned parallel to the flow direction (*e.g.*, Polo *et al.* 2018b, Benites *et al.* 2020). *Ram* amygdales are mostly filled with chalcedony, while in intensely altered *Ral*, they are filled with clay materials (Fig. 3C). In *Ral*, amygdales tend to aggregate locally, forming centimetric pockets.

Morphology of volcanic bodies

Due to the local relief, a careful stratigraphic control and detailed geological mapping are hampered by the kilometric distances that usually separate outcrops. Moreover, stratigraphic

Table 1. Main features of the Palmas lithofacies described in the study area. Modal proportions obtained by visual estimation.

Lithofacies		Structures	Mineral assemblage and glassy matrix (vol.%)					
			pl	px	opa	apa	mat	gl
Rb	compositionally banded rhyolite	flow banding; local amygdales	15-25	tr.-10	tr.-5	tr.	20-40	35-45
Rvb	banded vitreous rhyolite	flow banding; local amygdales	10	10	5	0	0	75
Rd	rhyolite with planar disjuctions	planar disjunctions; local amygdales	10-30	tr.-10	tr.-10	tr.	25-65	10-50
Raf	aphanitic rhyolite	planar disjunctions; local amygdales (flow banding)	15-25	tr.-10	5-10	tr.	5-10	55-75
P	Pitchstone	planar disjunctions; amygdaloid (ca. 15%)	10-20	tr.-10	tr.-10	tr.	0-5	65-80
Ram	amygdaloid rhyolite	planar disjunctions; amygdaloid (ca. 30%)	15-20	5-10	tr.-10	0	0	65-70
Ral	altered rhyolite	planar disjunctions; flow banding; amygdaloid (up to 35%);	15-20	?	?	?	80-85	
Rq	rhyolite with quartz levels	planar disjunctions; quartz levels	15	5	10	tr.	55	15
Rm	massive rhyolite	massive	20-25	5-10	5	tr.	20-30	40

Pl: plagioclase; px: pyroxene; opa: opaques; apa: apatite; mat: quartz-feldspar matrix; gl: glassy matrix.
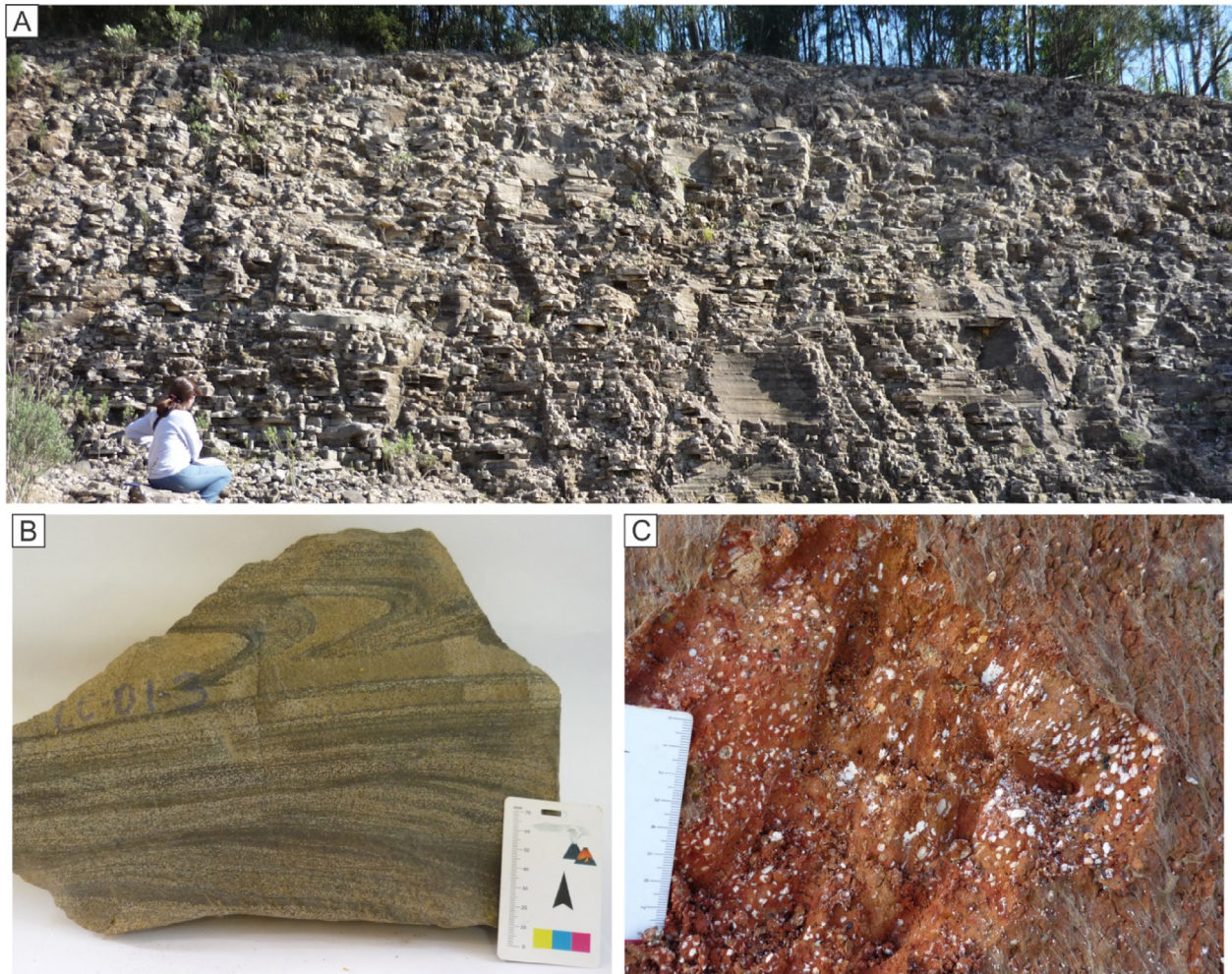
Figure 3. (A) Overview of outcropping *Rd* rocks (PAL28) with centimetric planar disjunctions; (B) *Rb* sample with compositional banding forming intrafolial folds (PAL01); (C) *Ral* outcrop with clay mineral-filled amygdales (PAL32).

correlation based solely on topographic gaps would be an inaccurate and simplistic approach to take, given the small (1°-2°) regional NNW dip and shear zones that affect the rocks. However, individual volcanic bodies and stacking relations can be observed at outcrop scale, as described below.

Lobes

Meter-scale lobes (average height of 8 m) are observed, usually with flanks at about 55° dip angles and varying flow directions. *Rd* is the most common lithofacies forming these bodies, occurring either restricted to their cores (Fig. 4A) or composing the entire lobe (Fig. 4B). In the first case, the external carapace is formed by *Ral*, whose intensely stretched amygdales (up to 30%) follow the boundaries of the preserved core, concentrated in the basal and lateral portions of the lobe. At the basal portions, the planar disjunctions are tighter. Discontinuous veins concordant with the core and filled with clay minerals are common. Regardless of lithofacies, planar disjunctions are concordant with lobe boundaries. Locally, an oligomitic breccia is observed at the contact between *Rd* and *Ral* (Fig. 4C), yielding sub-rounded *Rd* clasts sustained by a *Ral* matrix. Occasionally, *Raf* and *P* occur below *Rd* or covering the lobe, respectively.

Tabular bodies

The extensive tabular bodies (decametric thickness) observed in the area are mainly composed of *Rd*. Their planar disjunctions are largely horizontal, but very local truncation or mild undulation are also observed. The upper portions of the tabular bodies are marked either by the presence of *P* or by *Rd* with columnar disjunctions (Fig. 5A). In the latter, tight planar disjunctions (up to 5 cm, near the top of the sequence) gradate to more spaced disjunctions until they reach decimetric thicknesses in the middle portion of the sequence (Fig. 5B). At some outcrops, the basal parts of the body are formed by *Ral*, with flat amygdales occupying up to 15% of the rock volume. In some places, *Rq* lies above *Ral*, the latter showing a folded compositional banding that is cut by clay mineral-filed veins.

Volcanic conduits

At some outcrops, lateral variation from *P* through *Raf* to *Rd* and from *Raf* to *Rd* are associated with vertical planar disjunctions (Fig. 6), a sequence interpreted as volcanic conduits. The glassy content decreases toward the central portions of such structures. Locally, a network of *Raf* dykes and sills (of centimetric thickness) is intruded into *Rd*.
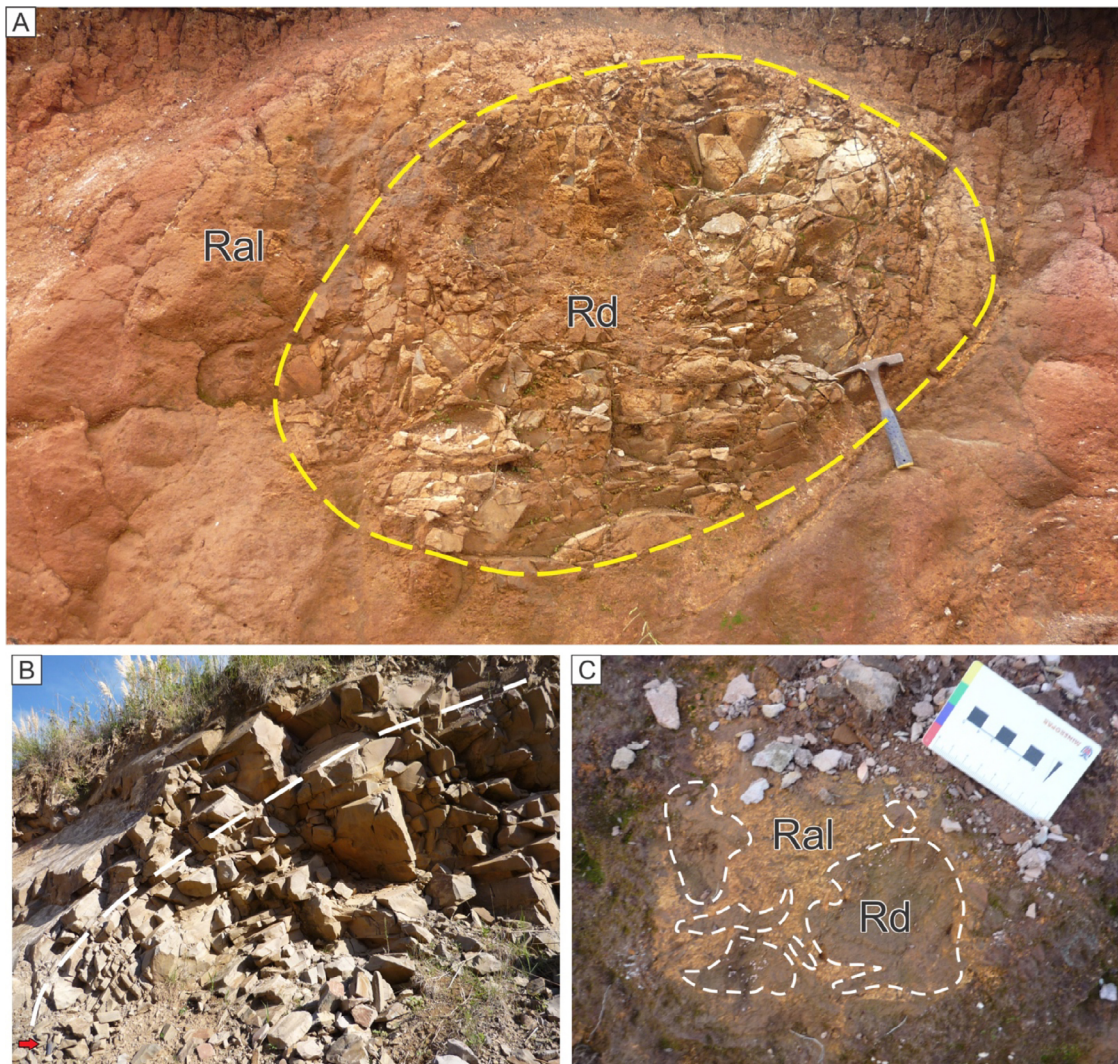
Figure 4. (A) Lobe with a *Rd* core and *Ral* carapace (PAL33); (B) Lobe consisting entirely of *Rd* (PAL54); (C) Breccia with *Rd* clasts surrounded by an *Ral* matrix (PAL33).
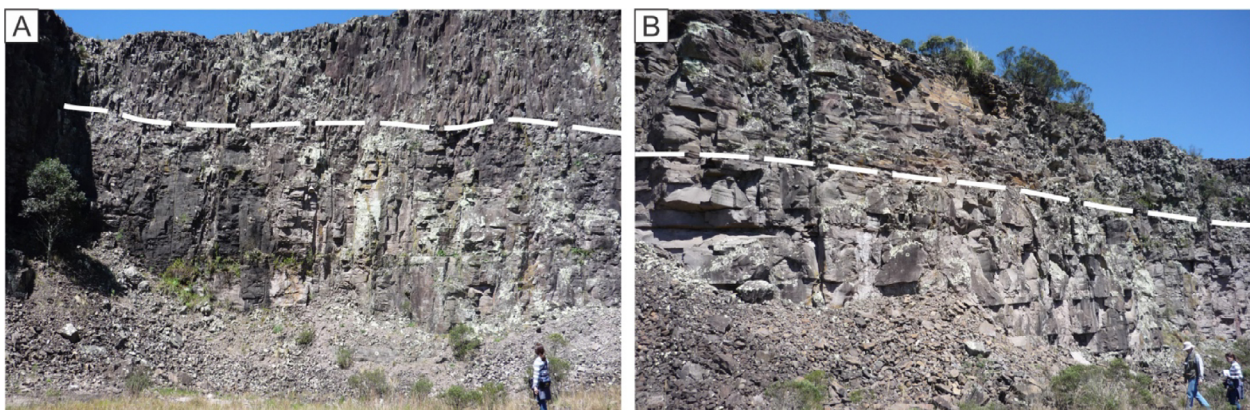
Figure 5. Tabular unit (PAL11) composed of *Rd* showing (A) columnar disjunctions and (B) tight to decimetric planar disjunctions.

Petrography

Petrographic analysis reveals that the investigated lithofacies show little difference in terms of mineral assemblage, only modal variations in the proportion of each crystalline phase. Thus, as evidenced in macroscopic analysis, lithotypes are mainly identified based on textural and structural features and on the amount of volcanic glass. Although characterized as aphyric in hand samples, the rocks consist of plagioclase and pyroxene microphenocrystals surrounded by a groundmass made of volcanic glass (in different stages of devitrification) and crystals of alkaline feldspar, quartz, apatite, and opaques (Fig. 7A).

Figure 6. Volcanic conduit (PAL16) indicated by vertical planar disjunctions (highlighted in yellow) from which a network of dykes and sills (gray) intrudes into *Rd* (horizontal disjunctions in blue).
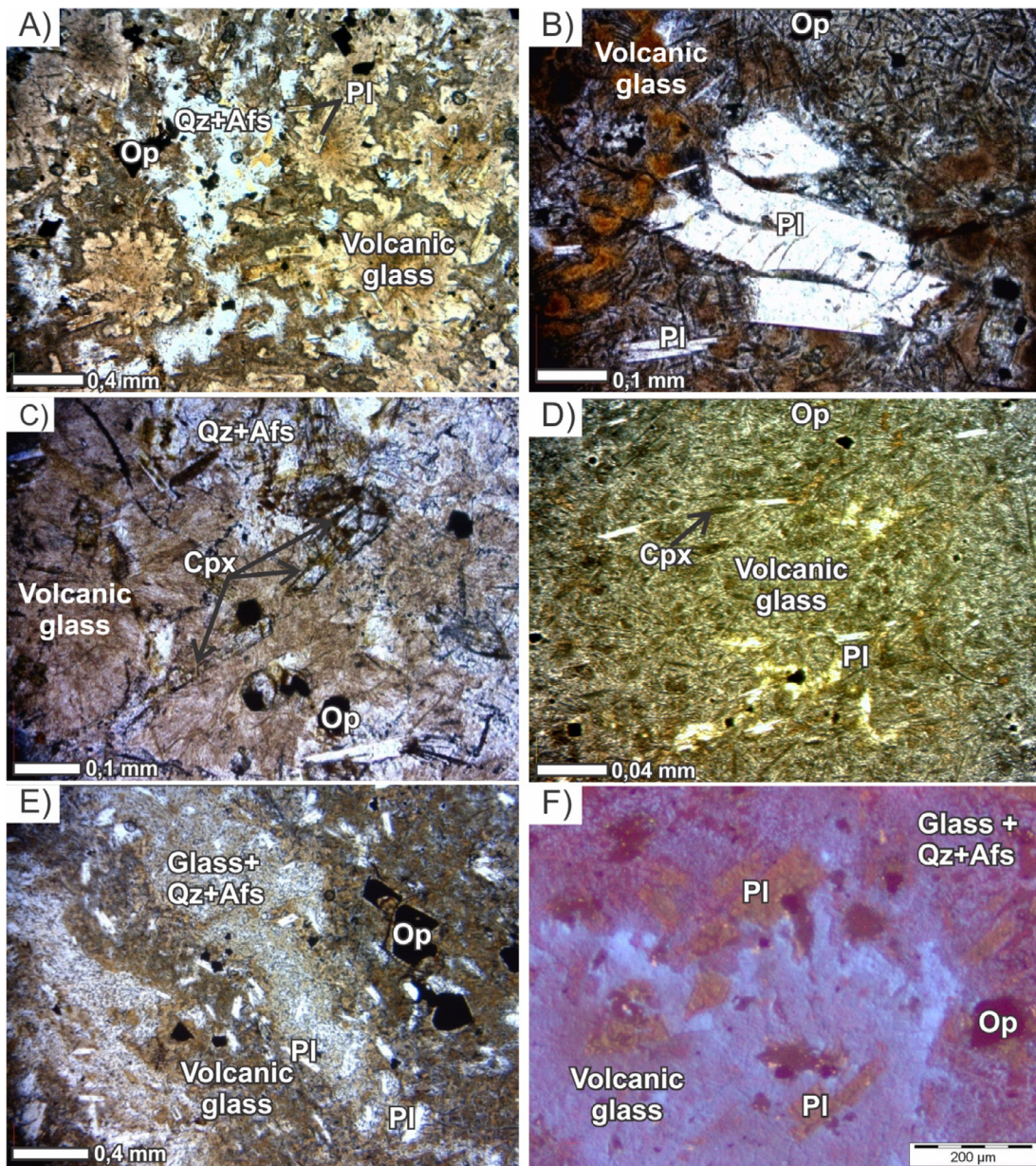
Qz: quartz; Afs: alkaline feldspar; Pl: plagioclase; Cpx: clinopyroxene; Op: opaque minerals. Photomicrographs under natural light.
Figure 7. Overview of the lithotypes present in the Palmas plateau: (A) plagioclase microphenocrysts in quartz-feldspar matrix and volcanic glass (PAL27); (B) microphenocrysts of slightly flexed plagioclase amid vitreous matrix with perlitic cracks (PAL25); (C) microphenocryst of fractured Ca-clinopyroxene in quartz-feldspar matrix and volcanic glass (PAL01); (D) hypohyaline microporphitic texture in pitchstone (PAL33); (E) aphanitic rhyolite with compositional banding (PAL16); (F) detail of compositional banding under cathodoluminescence (PAL01).

According to Energy-Dispersive X-Ray Spectroscopy (EDS) analyses, plagioclase presents similar percentages of Na_2O and CaO, with a slightly higher Na_2O peak, and therefore is identified as andesine. Plagioclase occurs as microlites (< 25 vol.%) and microphenocrysts (up to 5 vol.%), the latter with euhedral and subhedral forms. Plagioclase is parallel to both compositional banding and planar disjunctions, defining magmatic flow structures. Subordinated zoned crystals with swallowtail terminations (up to 0.5 mm) are engulfed by the vitreous matrix. Broken or slightly flexed microphenocrysts are locally present (Fig. 7B). Alteration of plagioclase to white mica ranges from incipient to intense.

Pyroxene corresponds to a maximum 10 vol.% of the modal composition, but may also occur in trace amounts. In some places, hollow acicular crystals indicate rapid crystallization. Similarly to plagioclase, broken pyroxene is also present (Fig. 7C). EDS does not reveal significant Ca peaks, which allows the mineral to be identified as a Ca-poor clinopyroxene (pigeonite) or orthopyroxene.

Very fine crystals of quartz and alkaline feldspar form the crystalline matrix, here referred to as quartz-feldspar matrix (5 to 65 vol.%). The habit of these two minerals is anhedral, with poorly defined and sometimes anastomosed borders.

Fined-grained, euhedral to subhedral primary opaque minerals with square or triangular sections make up < 10 vol.% of the rocks. Accessory apatite is present as very thin prismatic or hexagonal euhedral crystals. The secondary mineral assemblage is formed by the sericite, opaque minerals, and restricted chlorite. Although these minerals also fill amygdales, in general they are found replacing primary phases.

Regarding texture, the lithofacies differ among themselves in the degree of devitrification, which ranges from 10 to 80 vol.%, forming hypocrystalline or hypohyaline textures (Figs. 7A and 7D, respectively). The glass, dark reddish-brown to pale yellowish-brown in color, is isotropic or, where in initial stages of devitrification, slightly birefringent. Among the devitrification features observed are perlitic cracks (Fig. 7B) and spherulites.

Among the volcanogenic structures described in the field, the banded flow is microscopically defined by levels of different colors of volcanic glass and variations in the amount of quartz-feldspar matrix (Fig. 7E). While the macroscopically dark greenish-gray levels consist predominantly of medium brown volcanic glass (65 vol.%), light greenish-gray levels consist of pale yellowish-brown volcanic glass (45 vol.%). Cathodoluminescence analysis indicates variations in luminescense patterns between levels, dark bands being predominantly blue and light ones reddish (Fig. 7F). Such a response indicates compositional variation, since blue light results from structural defects normally related to $Al-O^--Al$ bonds while red components are indicative of Eu^{2+}, Fe^{3+} or Ti^{4+} in the alkaline feldspar structure (Götze *et al.* 2000).

A second type of banded structure is observed in *Rvb*. It differs from the one described above in the larger presence of volcanic glass and in the wider variety of band types (A, B, C, D, and E, each one characterized by different proportions of constituents — Fig. 8A, Tab. 2). All layers consist of
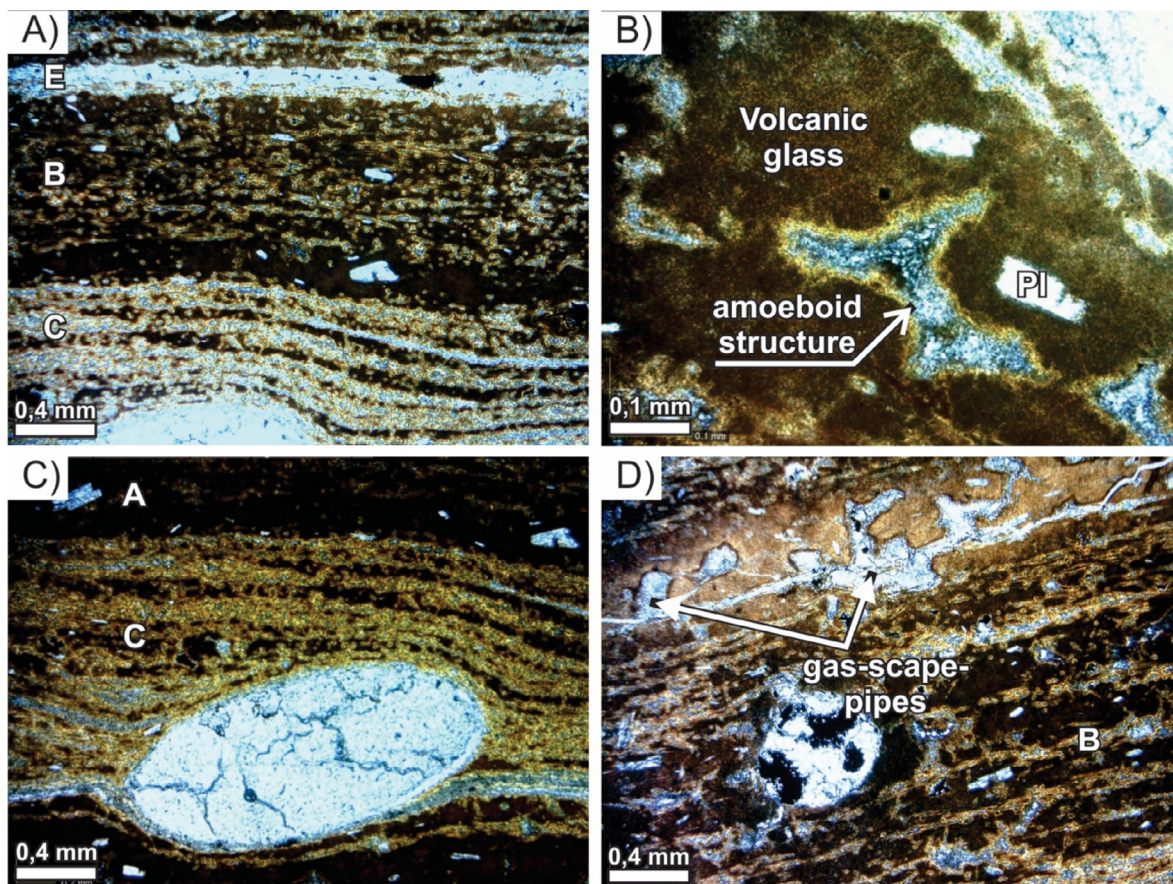
Figure 8. Particular features of the *Rvb* lithofacies (PAL34): (A) Compositional banding; (B) Amoeboid volcanic glass; (C) Rotated amygdale; (D) gas-escape-pipes. Photomicrographs under natural light.

Table 2. Main features of the Rvb lithofacies. Modal proportions obtained by visual estimation.
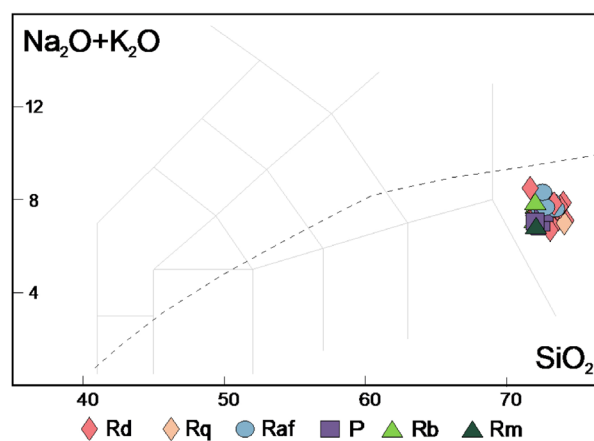
Layer	Composition	Particular features
A	Volcanic glass (90 vol.%: 70 vol.% gl, 10 vol.% Mam and 10 vol.% Fam) and plagioclase (10 vol.%)	–
B	Volcanic glass (85 vol.%: 55 vol.% gl, 5 vol.% Mam and 25 vol.% Fam), pyroxene (5 vol.%) e opaques (tr.)	Locally discontinuous layers
C	Volcanic glass (90 vol.%: 15 vol% gl and 85 vol.% Fam), pyroxene (5 vol.%), opaques (5 vol%) and plagioclase (tr.)	Locally discontinuous layers; Rotated amygdales and plagioclase.
D	Volcanic glass (65 vol.%: 40 vol.% gl, 20 vol.% Fam and 5 vol.% Fam), pyroxene (30%), opaques (5 vol.%) and plagioclase (tr.)	Rotated opaques; gas-escape-pipes
E	Quartz (75 vol.%), pyroxene (15 vol.%) and opaques (10 vol.%).	–

Gl: glassy matrix; Mam: medium-grained amoeboid structures; Fam: fine-grained amoeboid structures.

Figure 9. Palmas plateau rocks classified according the TAS diagram ($(Na_2O + K_2O)$ vs. SiO_2) of Le Maitre *et al.* (1989). Dashed line indicates the SiO_2 saturation limit in accordance with Irvine and Baragar (1971).


an association of glassy matrix and plagioclase, intensely oriented pyroxene, opaques, quartz, and amoeboid volcanic glass. The amoeboid glass (Fig. 8B) shows rounded terminations similar to fragmented vesicle walls and reaction borders with the surrounding vitreous matrix. Two grain-size populations occur: one with 0.2 mm (medium-grained) and another one with 0.01 mm (fine-grained) mean diameter. In some cases, cores are filled with secondary quartz. The different layers do not show any preferred distribution, are randomly arranged, and have gradational contacts between them, marked by variations in the proportions of the amoeboid structures. The banding forms close folds and, at some levels, amygdales (Fig. 8C) and minerals (opaque at level D and plagioclase at C) are rotated. Locally, portions of quartz levels are intrusive into the glassy matrix (Fig. 8D).

Geochemistry

Major and trace element analyses are presented as Supplementary Material B. Once TiO_2 contents are below 0.86 wt.%, the rocks are chemically defined as low TiO_2 Palmas-type. They correspond to the Clevelândia subtype following the criteria of Nardy *et al.* (2008), or to the Type 9 (high SiO_2 and low Zr, TiO_2, and P_2O_5) in the classification of Licht (2018). In the total alkali-silica (TAS) diagram (Fig. 9), the rocks are classified as rhyolite. In the multi-elemental diagrams (Fig. 10), negative anomalies of Ba, Sr, and Ti, and a positive anomaly of Pb are observed. As to the rare earth elements, enrichment in light rare earth elements (LREE) compared to heavy rare earth elements (HREE) is evidenced, except in two *Rb* samples. All rocks show negative Eu anomalies.
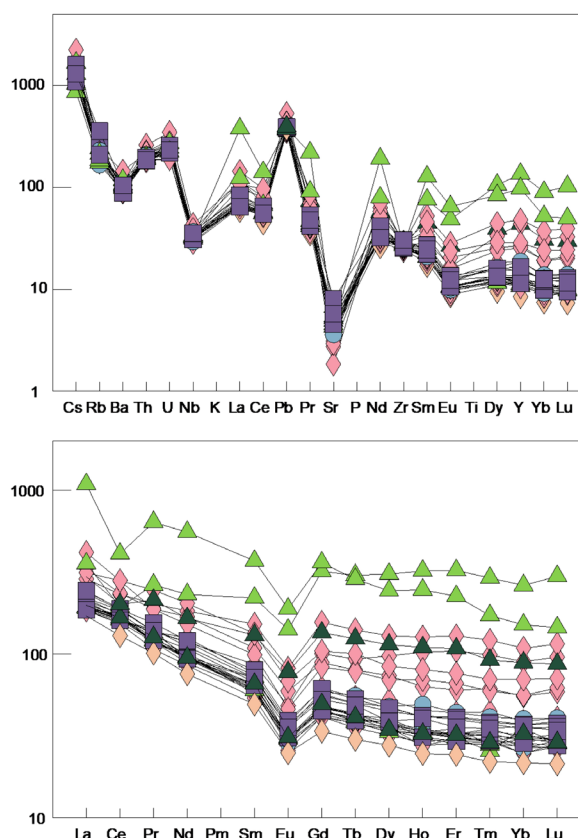
Figure 10. Primitive-mantle normalized (Sun and McDonough 1989) trace-element and (B) Chondrite-normalized (Sun and McDonough 1989) REE signatures for the studied rocks. Symbols as in Figure 9.

DISCUSSION

Effusive processes and the nature of the Palmas-type rocks

Discussion on the origin of Palmas-type rocks dates back to the pioneering mapping and geochemical characterization studies of the PIP (*e.g.*, Bellieni *et al.* 1986). However, it was only in the last decade, based on physical volcanology criteria, that more robust models were proposed (Waichel *et al.* 2012, Lima

et al. 2012, Polo and Janasi 2014, Polo et al. 2018a, 2018b, Besser et al. 2018, Luchetti et al. 2018a, 2018b, Guimarães et al. 2018a, 2018b, Benites et al. 2020). Luchetti et al. (2018b) indicated a pyroclastic origin for Palmas-type rocks that occur in central parts of the PIP (including those described in southwestern Paraná State), characterizing them as high-grade ignimbrites. Polo et al. (2018b), in turn, describe several structures indicative of effusive origin for Palmas volcanites that outcrop in the Gramado Xavier region, Rio Grande do Sul: lava domes, lobed flows, tabular flows, and basal autobreccias. All these structures are also observed in the Palmas plateau.

In fact, in addition to corroborating a high viscosity flow origin, the presence of lobes reinforces the effusive nature of the studied lithotypes. Manley (1996) considers the genesis of well-defined lobes inconsistent with a rheomorphic origin, especially in the vicinities of volcanic conduits. In this sense, Branney et al. (2004) take the absence of lobes in Grey's Landing rocks as diagnostic criteria for ignimbritic rather than effusive origin. In turn, such structures corroborate the effusive nature of the Snake River rhyolites according to Bonnichsen and Kauffman (1989). Some facies of the ideal dome models are not observed on the Palmas plateau (e.g., spherulitic horizons, pumice horizons, and obsidian from McPhie et al. 1993). According to Richnow (2000), the presence or absence of a given facies is determined by morphological (e.g., dome height and diameter) and cooling rate variations. Therefore,

even the flow lobes consisting exclusively of Rd (Fig. 4B) could be referred to as domes, given their restricted dimensions.

In several outcrops where lobes are absent, however, locally truncated planar disjunctions form tabular units of varying thickness. In view of this, the lava is considered to have reached the surface as extensive flows. Similarly, Besser et al. (2018) describe Palmas-type tabular bodies up to 40 km long and 100 m thick in São Joaquim, Santa Catarina. By proposing an effusive origin for these units, those authors argue that high effusion rates and continuous lava flow are determining factors in the generation of such expressive silicic units.

Field observation leads to the proposed lithofaciological sequence model for the Palmas rocks of southwestern Paraná depicted in Figures 11 and 12. Most facies described as flow lobes also occur as tabular bodies. In general, the faciological sequence involves, from bottom to top: an intensely altered rhyolitic level (Ral) with numerous amygdales and, occasionally, folded compositional banding; Raf or Rd, both with tightly-spaced planar disjunctions that scale to monotonous Rd levels with decimetric-spaced planar disjunctions and top portions with fast cooling rate features, such as tight planar disjunctions in Rd, columnar disjunctions, Ral, Ram or capping P.

The reason for the absence of basal autobreccia in the tabular units is still uncertain and may be due to burial, erosion, or some rheological particularity of the silicic lava. Henry and Wolff (1992) consider that the absence of basal breccia
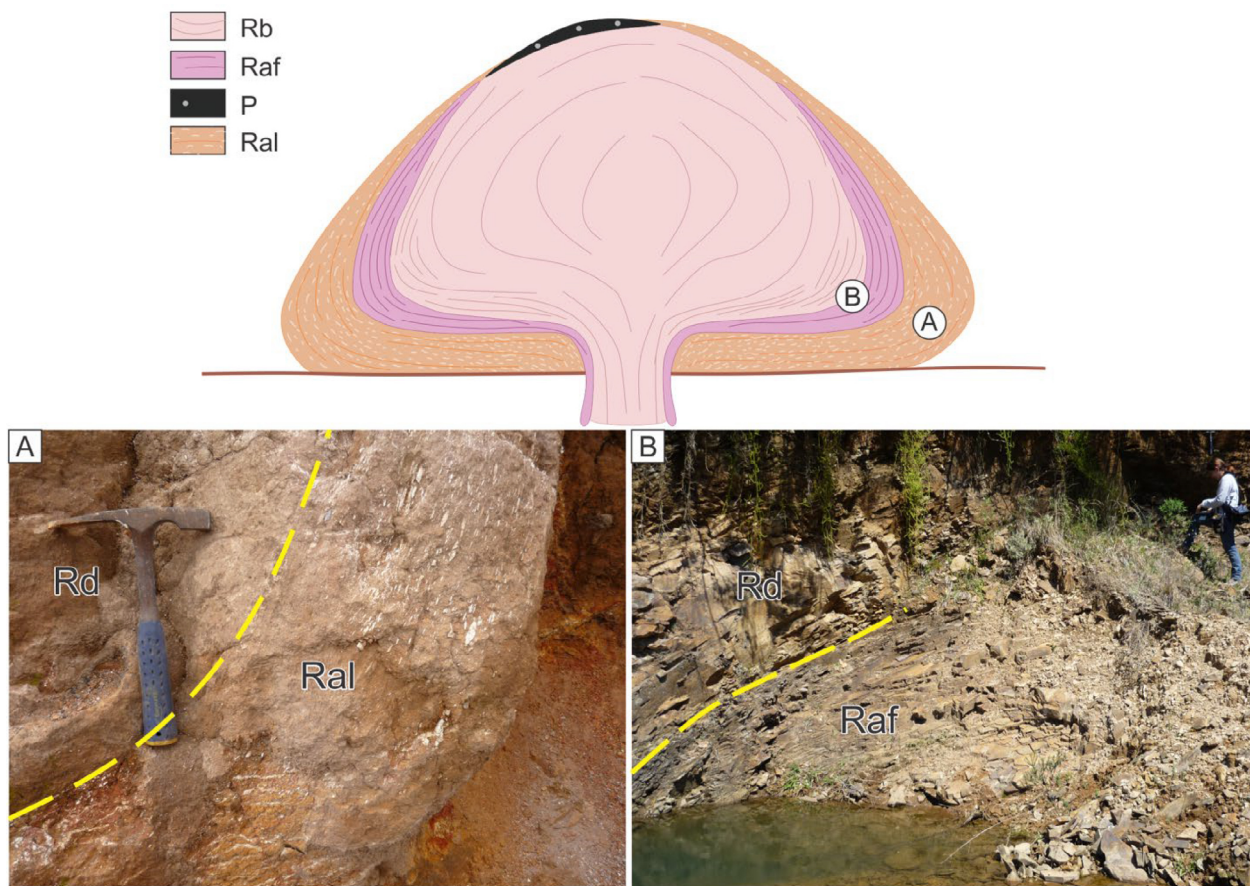
Figure 11. Schematic model for the ideal rhyolitic domes from the investigated area. In detail, (A) amygdales whose orientations change according to lobe shape (PAL33) and (B) contact between Raf and Rd (PAL26).

Figure 12. Schematic model for the tabular units from the investigated area. In detail, (A) *P* covering a tabular unit (PAL22); (B) thickness variation of planar disjunctions in *Rd* (PAL11); (C) contact between *Rd* and *Ral* at the base of a tabular unit (PAL20) and (D) altered compositional banding in *Ral* (PAL10).

is no unquestionable evidence of pyroclastic origin of a volcanic sequence, pointing out that in several provinces, particularly where magmatism reached high temperatures (such as in Palmas-type rocks, according to Nardy 1995, Simões *et al.* 2018, and Polo *et al.* 2018a), the presence of basal autobreccia is less common given the likely low viscosity of the lava. Once such breccias are present in basal portions of rhyolitic domes (Fig. 4C), it is assumed that the effective lava viscosity in these bodies was comparatively higher than in tabular ones. Moreover, being systematically found at the base of silicic units, *Ral* bears a more expressive amygdales volume where associated with domes than with tabular bodies. Thus, larger amounts of fluids exsolved from silicic melt (and therefore higher effective viscosity) may be one of the factors that defined the domic or tabular shapes.

Ram seems not to bear contact relations to other lithofacies. However, as this lithotype occurs at higher topographic levels (outcrops PAL12 and PAL13, between 1,284 and 1,299 m high) than nearby outcropping lithofacies (maximum 1,270 m high),

it is suggested that *Ram* may correspond to the top of a volcanic sequence, which is compatible with fast cooling rates. Thus, as vesicles expand toward the surface of the dome or effusive body, a surface is formed with small elongated vesicles and amygdales (ca. 25 to 40 vol.%) (Richnow 2000). Such characteristics are very similar to those observed in the amygdaloidal rhyolite, namely millimetric to centimetric oval and flat amygdales reaching 30 vol.%.

Rb occurs over *Rm*, forming the top of this volcanic sequence. In the tabular units, lithofacies *Rb* lies atop of *Rm*. According to Gregg *et al.* (1998), as the lava flow advances, its upper portion, colder due to contact with the atmosphere, tends to undergo compressional deformation generating folds, whose axes are perpendicular to the flow direction. Where compositional banding is present, folding is possible due to rheological contrast between levels of different compositions. Castro and Cashman (1999) observed that folded planes always show fewer vesicles than their surrounding matrix, which indicates that less viscous levels tend to bend over more viscous ones.

For the folded banding rhyolites from the studied area, rheological differences are due to variation between crystalline and melt proportions immediately after lava extrudes. Despite the small variation in microphenocryst content at both levels, and considering the quartz-feldspatic matrix as a primary one, light-colored levels consist of a 45 vol.% glassy to 55 vol.% crystalline composition, while in dark levels the proportions are of 65 vol.% glassy to 35 vol.% crystalline. The presence of crystals increases melt viscosity, thus defining the rheological contrast between levels.

Feeder conduits

Waichel *et al.* (2012) suggest that many conduits were required to generate the lava dome-field of Palmas-type described in the Torres Syncline region. Additionally, Polo *et al.* (2018b) propose that the numerous dome structures in Palmas-type rocks indicate that lava feeding took place just below these units. In the study area, lateral gradation from *P* through *Raf* to *Rd,* associated with the vertical planar disjunctions (Fig. 6), indicate lateral faciological variations across feeder conduits. *Raf* would, therefore, correspond to a transitional lithofacies between border (*P*) and core (*Rd*) portions of a conduit, with intermediate degrees of crystallinity. The metric to decametric distances between these lithofacies are indicative of conduit thickness.

According to Richnow (2000), several authors suggest that igneous banding in volcanic conduits is generated during magma ascension and flow. Thus, the shearing along the conduit walls forms almost vertical planes, as observed among the Palma-type rocks; as the lava flow advances and extrudes on the terrain, such structures become parallel to the paleosurface. Therefore, rhyolitic banding normally dips toward the conduit (Richnow 2000). Folded compositional banding, mostly intrafolial, can occur in *Raf* lithofacies associated with volcanic conduits (Fig. 7E, outcrop PAL16). Such features attest to the predominantly effusive origin of the Palmas-type rocks of southwestern Paraná as, according to Andrews and Branney (2011), rheomorphic ignimbrites do not preserve shear features near conduits due to intense fragmentation during the pyroclastic flow. In contrast, those authors point out that silicic effusive rocks can generate flow bands, folds and stretching lineations even in areas near the conduits. Folding is possible once lava travels mostly as a ductile flow. Conversely, pyroclastic flows are only able to generate folds during final flow stages, at the more distal flow portions and far away from the conduits (Andrews and Branney 2011).

Localized piroclastic processes

Rvb (outcrop PAL34) has particular characteristics that do not fit to a lava solidification an origin. Its amoeboid volcanic glass structures resemble fragmented vesicle walls, which allows them to be referred to as shards. According to McPhie *et al.* (1993), the term identifies particles generated by either explosive or non-explosive fragmentation of magma or lava during rapid cooling, or friction between glassy clasts during transport. For Henry and Wolff (1992), the presence of pumice or shard only indicates vesiculation and fragmentation of the magma, which does not necessarily imply pyroclastic origin. However, these authors emphasize that, in effusive rocks, shard is associated with top, bottom or marginal flow breccia, whereas in rheomorphic ignimbrites it can be present in any area of the deposit.

Rvb overlies *Ral* without any evidence of interaction between both lithofacies, which allows disregarding the former as a basal flow breccia. Andrews and Branney (2011) also consider that shards associated with effusive autobreccias are normally sheared, while those of pyroclastic origin retain shape, be it the original or a cuspate shape, as seen in *Rvb*. The presence of rotated minerals and amygdales also suggests a different rheological behavior than other investigated effusive lithofacies with flow banding. The presence of close folds is made possible by compositional variations that determine a different rheological behavior for each lithofacies level.

Also, the gradual contacts between *Rvb* levels are indicative of gradational bedding. In view of Henry and Wolff's (1992) reasoning that effusive deposits normally show vertical homogeneity while rheomorphic ignimbrites are heterogeneous, this could be evidence of pyroclastic origin. The described intrusive quartz levels suggest escape of volatile material, possibly through small *gas-escape pipes*, which, according to the same authors, are unique features of rheomorphic ignimbrites and, therefore, absent in silicic effusive rocks.

According to Fink and Manley (1989), volatile content increases substantially as the silicic lava flow advances, due to vapor migration and concentration after crystalline phase generation and microfracturing. For Henry and Wolff (1992), silicic lava fronts can collapse exposing the interior parts of volatile-supersaturated flows, which results in explosions that cause secondary pyroclastic flows. Deposits formed by such flows can be melted by the associated silicic lava (still advancing) to form rheomorphic-like features (Henry and Wolff 1992). It should also be noted that lobes (location PAL35) outcrop nearby *Rvb*.

Given the restricted occurrence of *Rvb*, we favor the hypothesis that this lithofacies may have resulted from a local pyroclastic flow, possibly related to silicic lava collapse. However, several features indicative of high- to extremely high-grade ignimbrites are reported by Luchetti *et al.* (2018b) in central PIP (surrounding our studied area), allowing these authors to propose an origin by pyroclastic fountaining eruptions. Therefore, further studies are necessary to better constrain the exact origin of this particular lithofacies.

CONCLUDING REMARKS

The rhyolitic domes and tabular units that occur on the Palmas plateau in southeastern Paraná State were predominantly generated by effusive processes. As their important lithofaciological variations, mainly regarding textures and structures, occur in an organized manner in each volcanic body, stacking/zoning models can be proposed. Only one pyroclastic lithofacies is described in the study area (*Rvb*), presenting shards, gradational bedding and gas-escape pipes, indicative of rheomorphism. However, the restricted occurrence

of this lithofacies suggests origin from an equally localized event. Therefore, secondary pyroclastic flows resulting from the collapse of the silicic lava front are considered. Lava may have generated rheomorphic features while still in motion, although further studies are suggested to better constrain the exact origin of this particular lithofacies.

ACKNOWLEDGMENTS

REFERENCES

Andrews G.D.M., Branney M.J. 2011. Emplacement and rheomorphic deformation of a large rhyolitic ignimbrite: Grey's Landing, southern Idaho. *Bulletin of Geological Society of America*, **123**(3-4):725-743. https://doi.org/10.1130/B30167.1

Bellieni G., Comin-Chiaramonti P., Marques L.S., Melfi A.J., Nardy A.J.R., Papatrechas C., Piccirillo E.M., Roisenberg A. 1986. Petrogenetic aspects of acid and basaltic lavas from the Paraná plateau (Brazil): geological, mineralogical and petrochemical relationships. *Journal of Petrology*, **27**(4):915-944. https://doi.org/10.1093/petrology/27.4.915

Bellieni G., Comin-Chiaramonti P., Marques L.S., Melfi A.J., Piccirillo E.M., Nardy A.J.R., Roisenberg A. 1984. High-and low-TiO2 flood basalts from the Paraná plateau (Brazil): petrology and geochemical aspects bearing on their mantle origin. *Neues Jahrbuch für Mineralogie Abhandlungen*, **150**(3):273-306.

Benites S., Sommer C.A., Lima E.F., Savian J.F., Haag M.B., Moncinhatto T.R., Trindade R.I.D. 2020. Characterization of volcanic structures associated to the silicic magmatism of the Paraná-Etendeka Province, in the Aparados da Serra region, southern Brazil. *Anais da Academia Brasileira de Ciências*, **92**(2):e20180981. https://doi.org/10.1590/0001-3765202020180981

Besser M.L., Vasconcellos E.M.G., Nardy J.A.R. 2018. Morphology and stratigraphy of Serra Geral silicic lava flows in the northern segment of the Torres Trough, Paraná Igneous Province. *Brazilian Journal of Geology*, **48**(2):201-219. https://doi.org/10.1590/2317-4889201820180087

Bonnichsen B., Kaufmann D.F. 1989. Physical features of rhyolite lava flows in the Snake River Plain volcanic province, southwestern Idaho. *Geological Society of America Special Paper*, **212**:119-145. https://doi.org/10.1130/SPE212-p119

Branney M.J., Barry T.L., Godchaux M. 2004. Sheathfolds in rheomorphic ignimbrites. *Bulletin of Volcanology*, **66**(6):485-491. https://doi.org/10.1007/s00445-003-0332-8

Branney M.J., Kokelaar B.P. 1992. A reappraisal of ignimbrite emplacement: progressive aggradation and changes from particulate to non-particulate flow during emplacement of high-grade ignimbrite. *Bulletin of Volcanology*, **54**:504-520. https://doi.org/10.1007/BF00301396

Bryan S.E., Ewart A., Stephens C.J., Parianos J., Downes P.J. 2000. The Whitsunday Volcanic Province, Central Queensland, Australia: Lithological and stratigraphic investigations of a silicic-dominated large igneous province. *Journal of Volcanology and Geothermal Research*, **99**(1-4):55-78. https://doi.org/10.1016/S0377-0273(00)00157-8

Castro J.M., Cashman K.V. 1999. Constraints on rheology of obsidian and pumice based on folds in obsidian lavas. *Journal of Structural Geology*, **21**(7):807-819. https://doi.org/10.1016/S0191-8141(99)00070-X

Fink J.H., Manley C.R. 1989. Explosive volcanic activity generated within advancing silicic lava flows. In: Lauer J. (ed.). *Volcanic Hazards*. International Association of Volcanology and Chemistry of the Earth's Interior, p. 169-179.

Frank H.T., Gomes M.E.B., Formoso M.L.L. 2009. Review of the areal extent and the volume of the Serra Geral Formation, Paraná Basin, South America. *Pesquisas em Geociências*, **36**(1):49-57.

Garland F., Hawkesworth C.J., Mantovani M.S.M. 1995. Description and Petrogenesis of the Paraná Rhyolites, Southern Brazil. *Journal of Petrology*, **36**(5):1193-1227. https://doi.org/10.1093/petrology/36.5.1193

Gomes A.S., Licht O.A.B., Vasconcellos E.M.G., Soares J.S. 2018. Chemostratigraphy and evolution of the Paraná Igneous Province volcanism in the central portion of the state of Paraná, Southern Brazil. *Journal of Volcanology and Geothermal Research*, **355**:253-269. https://doi.org/10.1016/j.jvolgeores.2017.09.002

Götze J., Krbetschek M.R., Habermann D., Wolf D. 2000. High-resolution cathodoluminescence studies of feldspar minerals. In: Pagel M., Barbin V., Blanc P., Ohnenstetter D. (eds.). *Cathodoluminescence in geosciences*. Berlin: Springer, p. 245-270.

Gregg T.K.P., Fink J.H., Griffiths R.W. 1998. Formation of multiple fold generations on lava flow surfaces: Influence of strain rate, cooling rate and lava composition. *Journal of Volcanology and Geophysical Research*, **80**(3-4):281-292. https://doi.org/10.1016/S0377-0273(97)00048-6

Guimarães L.F., Campos C.P., Janasi V.D.A., Lima E.F., Dingwell D.B. 2018a. Flow and fragmentation patterns in the silicic feeder system and related deposits in the Paraná-Etendeka Magmatic Province, São Marcos, South Brazil. *Journal of Volcanology and Geothermal Research*, **358**:149-164. https://doi.org/10.1016/j.jvolgeores.2018.03.021

Guimarães L.F., Raposo M.I.B., Janasi V.D.A., Cañón-Tapia E., Polo L.A. 2018b. An AMS study of different silicic units from the southern Paraná-Etendeka Magmatic Province in Brazil: Implications for the identification of flow directions and local sources. *Journal of Volcanology and Geothermal Research*, **355**:304-318. https://doi.org/10.1016/j.jvolgeores.2017.11.014

Henry C.D., Wolff J.A. 1992. Distinguishing strongly rheomorphic tuffs from extensive silicic lavas. *Bulletin of Volcanology*, **54**:171-186. https://doi.org/10.1007/BF00278387

Irvine T.N., Baragar W.R.A. 1971. A guide to the chemical classification of the common volcanic rocks. *Canadian Journal of Earth Sciences*, **8**(5):523-548. https://doi.org/10.1139/e71-055

Le Maitre R.W., Bateman P., Dudek A., Keller J., Lameyre J., Le Bas M.J., Sabine P.A., Schmid R., Sorensen H., Streckeisen A., Woolley A.R., Zanettin B.A. 1989. *Classification of Igneous Rocks and Glossary of terms:* Recommendations of the International Union of Geological Sciences Subcommission on the Systematics of Igneous Rocks. Oxford: Blackwell Scientific Publications.

Licht O.A.B. 2018. A revised chemo-chrono-stratigraphic 4-D model for the extrusive rocks of the Paraná Igneous Province. *Journal of Volcanology and Geothermal Research*, **355**:32-54. https://doi.org/10.1016/j.jvolgeores.2016.12.003

Licht O.A., Arioli E.E. 2018. *Mapa geológico do Grupo Serra Geral no estado do Paraná, escala 1:500.000*. Curitiba: Instituto de Terras, Cartografia e Geologia do Paraná.

Lima E.F., Philipp R.P., Rizzon G.C., Waichel B.L., Rosetti L.M.M. 2012. Sucessões Vulcânicas e Modelo de Alimentação e Geração de Domos de Lava Ácidos da Formação Serra Geral na Região de São Marcos-Antonio Prado (RS). *Geologia USP, Série Científica*, **12**(2):49-64. https://doi.org/10.5327/S1519-874X2012000200004

Luchetti A.C.F., Gravley D.M., Gualda G.A., Nardy A. J. 2018a. Textural evidence for high-grade ignimbrites formed by low-explosivity eruptions, Paraná Magmatic Province, southern Brazil. *Journal of Volcanology and Geothermal Research*, **355**:87-97. http://dx.doi.org/10.1016/j.jvolgeores.2017.04.012

Luchetti F., Nardy A.J.R., Madeira J. 2018b. Silicic, high- to extremely high-grade ignimbrites and associated deposits from the Paraná Magmatic Province, southern Brazil. *Journal of Volcanology and Geothermal Research*, **355**:270-286. https://doi.org/10.1016/j.jvolgeores.2017.11.010

Machado F.B., Rocha-Júnior E.R.V., Marques L.S., Nardy A.J.R., Zezzo L.V., Marteleto N.S. 2018. Geochemistry of the Northern Paraná Continental Flood Basalt (PCFB) Province: implications for regional chemostratigraphy. *Brazilian Journal of Geology*, **48**(2):177-199. http://dx.doi.org/10.1590/2317-4889201820180098

Manley C.R. 1996. Physical volcanology of a voluminous rhyolite lava flow: The Badlands lava, Owyhee Plateau, southwestern Idaho. *Journal of Volcanology and Geothermal Research*, **71**(2-4):129-153. https://doi.org/10.1016/0377-0273(95)00066-6

Marques S.L., Ernesto M.O. 2004. Magmatismo toleítico da Bacia do Paraná. In: Mantesso-Neto V., Bartorelli A., Carneiro C.D.R., Brito-Neves B.B. Geologia *do Continente Sul Americano:* Evolução da Obra de Fernando Flávio Marques de Almeida. São Paulo: Beca, p. 245-263.

McPhie J., Doyle M., Allen R. 1993. *Volcanic textures:* a guide to the interpretation of textures in volcanic rocks. Tasmania: University of Tasmania: Centre for Ore Deposit and Exploration Studies.

Melfi A.J., Piccirillo E.M., Nardy A.J.R. 1988. Geological and magmatic aspects of the Paraná Basin - an introduction. *In*: Piccirillo E.M., Melfi A.J. (eds.). *The Mesozoic flood volcanism of the Paraná Basin:* petrogenetic and geophysical aspects. São Paulo: Instituto Astronômico e Geofísico, p. 1-14.

Milner S. C., Duncan A. R., Ewart A. 1992. Quartz latite rheoignimbrite flows of the Etendeka Formation, north-western Namibia. *Bulletin of Volcanology*, **54**:200-219. https://doi.org/10.1007/BF00278389

Nardy A.J.R. 1995. *Geologia e petrologia do vulcanismo mesozóico da região central da Bacia do Paraná*. PhD Thesis, Instituto de Geociências e Ciências Exatas, Universidade Estadual Paulista "Júlio de Mesquita Filho", Rio Claro, 316 p.

Nardy A.J.R., Machado F.B., Oliveira M.A.F. 2008. As rochas vulcânicas mesozóicas ácidas da Bacia do Paraná: litoestratigrafia e considerações geoquímico-estratigráficas. *Revista Brasileira de Geociências*, **38**(1):178-195.

Németh K., Martin U. 2007. *Practical volcanology:* lectures notes for understanding volcanic rocks from field based studies. Budapest: Geological Institute of Hungary.

Peate D.W., Hawkesworth D.J., Mantovani M.M.S. 1992. Chemical stratigraphy of the Paraná lavas (South America): classification of magma types and their spatial distribution. *Bulletin of Volcanology*, **55**:119-139. https://doi.org/10.1007/BF00301125

Philipp R.P., Vieiro A.P., Neves P.C.P., Robaina L.E.S., Zanette I.L. 1994. Caracterização geológica e petrológica preliminar do vulcanismo ácido da região de Campos Novos, Santa Catarina. *Boletim IG-USP, Série Científica*, **25**:17-27. http://dx.doi.org/10.11606/issn.2316-8986.v25i0p17-27

Polo L.A., Giordano D., Janasi V.A., Guimarães L.F. 2018a. Effusive silicic volcanism in the Paraná Magmatic Province, South Brazil : Physico-chemical conditions of storage and eruption and considerations on the rheological behavior during emplacement. *Journal of Volcanology and Geothermal Research*, **355**:115-135. https://doi.org/10.1016/j.jvolgeores.2017.05.027

Polo L.A., Janasi V.A. 2014. Vulcano-estratigrafia das rochas intermediárias a ácidas ao sul da Província Magmática Paraná, Brasil. *Geologia USP, Série Científica*, **14**(2):83-100. http://dx.doi.org/10.5327/Z1519-874X201400020005

Polo L.A., Janasi V.A., Giordano D., Lima E.F., Cañon-Tapia E., Roverato M. 2018b. Effusive silicic volcanism in the Paraná Magmatic Province, South Brazil: Evidence for locally-fed lava flows and domes from detailed field work. *Journal of Volcanology and Geothermal Research*, **355**:204-218. https://doi.org/10.1016/j.jvolgeores.2017.08.007

Richnow J. 2000. *Eruptional and post-eruptional processes in rhyolite domes, vol. 2: Drafts of papers*. PhD Thesis, University of Canterbury, New Zeland, 49 p.

Roisenberg A. 1989. *Petrologia e geoquímica do vulcanismo ácido mesozóico da Província Meridional da Bacia do Paraná*. PhD Thesis, UFRGS, Instituto de Geociências, Porto Alegre, 285 p.

Rossetti L., Lima E.F., Waichel B.L., Hole M.J., Simões M.S., Scherer C.M. 2018. Lithostratigraphy and volcanology of the Serra Geral Group, Paraná-Etendeka Igneous Province in southern Brazil: Towards a formal stratigraphical framework. *Journal of Volcanology and Geothermal Research*, **355**:98-114. https://doi.org/10.1016/j.jvolgeores.2017.05.008

Serviço Geológico do Paraná (MINEROPAR). 2005. *Mapa Geológico da Folha de Clevelândia, Folha SG.22-Y-B, escala 1:250.000*. Curitiba: Minerais do Paraná S/A.

Simões M.S., Lima E.F., Sommer C.A., Rosseti L.M.M. 2018. The Mato Perso Conduit System: evidence of silicic magma transport in the southern portion of the Paraná-Etendeka LIP, Brazil. *Brazilian Journal of Geology*, **48**(2):263-281. https://doi.org/10.1590/2317-4889201820170080

Sun S.S., Mcdonough W.F. 1989. Chemical and isotopic systematics of oceanic basalts: implications for mantle composition and processes. *In*: Sauders M.J. *Magmatism in the ocean basins*. London: Geological Society Special Publications, p. 313-345. v. 42.

Umann L.V., Lima E.F., Sommer C.A., Liz J.D. 2001. Vulcanismo ácido da região de Cambará do Sul; RS: litoquímica e discussão sobre a origem dos depósitos. *Revista Brasileira de Geociências*, **31**(3):357-364.

Waichel B.L., Lima E.F., Viana A.R., Scherer C.M., Bueno G.V., Dutra G. 2012. Stratigraphy and volcanic facies architecture of the Torres Syncline, Southern Brazil, and its role in understanding the Paraná–Etendeka Continental Flood Basalt Province. *Journal of Volcanology and Geothermal Research*, **215-216**:74-82. https://doi.org/10.1016/j.jvolgeores.2011.12.004